

Phagocytized corpora amylacea as a histological hallmark of astrocytic injury in neuromyelitis optica.

Aya Suzuki¹, Hideaki Yokoo¹, Akiyoshi Kakita², Hitoshi Takahashi²,
Yasuo Harigaya³, Hayato Ikota¹, Yoichi Nakazato¹.

¹Department of Human Pathology, Gunma University Graduate School of Medicine, Maebashi, Japan

²Department of Pathology, Brain Research Institute, Niigata University, Niigata, Japan

³Department of Neurology, Maebashi Red-Cross Hospital, Maebashi, Japan

Running head title: phagocytized corpora amylacea in NMO

Correspondence to:

Hideaki Yokoo, MD, PhD

Department of Human Pathology, Gunma University Graduate School of Medicine

3-39-22, Showa, Maebashi, Gunma, 371-8511, Japan

Tel. (+81)-27-220-7971

Fax. (+81)-27-220-7978

e-mail. yokoo@med.gunma-u.ac.jp

* This work was supported in part by the Collaborative Research Project (2010-2215) of the Brain Research Institute, Niigata University, Japan.

* The authors declare no conflict of interest.

Abstract

Neuromyelitis optica (NMO) is an inflammatory demyelinating and necrotizing disorder of the central nervous system that mainly affects the optic nerve and spinal cord. The etiology is still uncertain; however, the discovery of serum anti-aquaporin-4 (AQP4) autoantibody is becoming the center of attention, and a new hypothesis is emerging that NMO is essentially astrocytopathy provoked by the autoantibody. In this study, we focused on corpora amylacea (CA), glycoproteinaceous inclusions in astrocytic processes. We examined 57 lesions in 9 cases of NMO spectrum disorder, and demonstrated that CA were phagocytized by macrophages in 42 lesions (74%) of 8 cases, while phagocytized figures were not seen in unaffected areas. Phagocytized CA were frequently encountered in early phase lesions still retaining myelin structures, while fewer or none were found in chronic destructive lesions. Moreover, phagocytized CA were significantly smaller in diameter than intact ones, and CA were decreased or absent in most lesions assessed. These findings suggest the following pathophysiological process: the astrocytes are affected at an early phase in NMO, CA are expelled from the astrocytes and phagocytized by macrophages finally leading to clearance. A phagocytized figure and subsequent loss of CA can be a histological hallmark of astrocytic injury of NMO.

Key words:

astrocytic injury, corpora amylacea, multiple sclerosis, neuromyelitis optica, phagocytosis.

INTRODUCTION

Neuromyelitis optica (NMO) is an inflammatory demyelinating and necrotizing disease of the central nervous system (CNS) mainly affecting the optic nerves and the spinal cord.^{1,2} There has long been controversy concerning whether NMO is a variant of multiple sclerosis (MS), called optic-spinal multiple sclerosis (OSMS) in Asian countries, or a distinct disease.^{3,4} Recently, an autoantibody reactive with structures adjacent to CNS microvessels, pia, subpia, and Virchow-Robin spaces was identified in sera of NMO as well as OSMS patients, and termed NMO-IgG.⁵ Subsequently, its relevant antigen turned out to be aquaporin-4 (AQP4), which is the main water channel protein in the CNS, densely expressed on astrocyte endfeet at the blood-brain barrier (BBB).⁶ In immunopathologic studies of NMO lesions, the immunoreactivity of AQP4 and glial fibrillary acidic protein (GFAP), an astrocyte-specific protein, was lost or diminished in the early stage of the lesions in NMO, especially in the perivascular areas with infiltration of T lymphocyte and activated complement and immunoglobulin deposition. On the other hand, the staining of myelin basic protein (MBP) was relatively preserved in acute inflammatory lesions. These features in NMO were not seen in MS lesions.^{7,8} Correlation of anti-AQP4 antibody titers with clinical severity of NMO,⁹ effectiveness of therapeutic removal of serum antibodies from NMO patients,¹⁰ and impairment of astrocytes both *in vitro* and *in vivo* by the patients' sera including anti-AQP4 antibody¹¹⁻¹⁴ are all indicative of pathogenicity of the autoantibody. Marked elevation of CSF levels of GFAP and S100 β during the acute phase of NMO also supports preferential astrocytic injury in the disease process.¹⁵⁻¹⁷ NMO can be distinguished from MS by clinical, neuroimaging and laboratory characteristics.¹⁸

Recently, we found interesting histopathological findings in an autopsy case of NMO spectrum disorder which had a very short clinical course of 27 days.¹⁹ In this case, inflammatory and necrotizing active lesions were found in the brainstem and spinal cord. In those lesions, myelinated fibers were relatively spared in spite of the loss or decreased expression of AQP4 and GFAP. These findings were consistent with a previous report of NMO.⁸ Notably, we found that corpora amylacea (CA) were phagocytized by macrophages in those lesions. To our knowledge, there is no such a previous report in NMO. CA are glycoproteinaceous inclusions and are most commonly located within astrocytes and their processes.²⁰ Here, we hypothesized that the astrocytes in the NMO lesions were affected primarily in the early phase of the disease, and then CA expelled from astrocytic processes. In the present study, we focused on phagocytized CA to investigate the significance in NMO.

MATERIALS AND METHODS

Tissue sample

Nine cases of neuropathologically-diagnosed NMO spectrum disorder were employed (Table 1).¹⁸ All patients showed preferential involvement of the spinal cord, medulla, and optic nerves. Some of the cases had already been reported elsewhere.^{8,19,21} All materials were obtained at autopsy. Tissue samples of the optic nerve, spinal cord and medulla oblongata were used for this study. The male to female ratio was 5:4, and median age was 69 (range 47-80) years. Disease duration ranged from 27 days to 40 years (median 8 years). Case 3 and 5 patients were seropositive for anti-AQP4 antibody and case 9 was

negative (courtesy of the Department of Neurology, Tohoku University, Sendai, Japan), while the other 6 cases were not examined.

Specimens were routinely formalin-fixed and paraffin-embedded. Five- μ m-thick sections were cut and stained with hematoxylin and eosin (HE) and Klüver-Barrera (KB). For immunocytochemistry, antibodies to CD68 (clone Ki-M1P, Seikagaku, Tokyo, Japan), AQP4 (polyclonal, Millipore, Billerica, MA), glial fibrillary acidic protein (GFAP),²² and myelin basic protein (MBP, Dako, Glostrup, Denmark) were used. Immunostaining for Schwann/2E²³ (Cosmo Bio, Tokyo, Japan) was performed on selected cases. This antibody specifically reacts with Schwann cells and myelin of the peripheral nervous system. For coloration, a commercially available biotin-streptavidin immunoperoxidase kit (Histofine, Nichirei, Tokyo, Japan) and diaminobenzidine were employed. Periodic acid-Schiff (PAS) was performed on the sections prestained by CD68, AQP4 or GFAP to highlight CA distribution and brain lesions. Because CA were dissolved and lost by heat treatment for antigen retrieval (data not shown), we selected Ki-M1P as a macrophage marker not requiring any pretreatment. The antibody is also demonstrated to stain macrophages most sensitively in the active MS lesion.²⁴

Neuropathological and immunohistochemical analysis

Firstly, we investigated the NMO lesions in 9 cases neuropathologically. For evaluation, morphologically-recognizable lesions such as demyelination, macrophage infiltration, necrosis, remyelination, and abnormal immunohistochemical staining were employed as indicators. All CNS lesions

were classified into 6 groups (patterns A-F) according to the expression patterns of AQP4, GFAP and MBP immunohistochemistry, as described by Misu et al. (Table 2).⁸ With regard to evaluation of AQP4, GFAP, and MBP immunohistochemistry, the lesions showing at least partial immunoreactivity were assessed as positive. Discontinuous lesions with the same expression pattern on an identical section were counted as one lesion. A continuous lesion having two or more expression patterns was counted as separate lesions. Consequently, we identified and assessed 57 lesions in total.

Phagocytized figures were classified in a two-tiered fashion as conspicuous and inconspicuous groups, according to the following definition: “conspicuous” was assigned when phagocytized figures were noticeable by HE specimen, while “inconspicuous” was selected when phagocytized CA were recognized only by CD68-PAS double staining. The diameter of phagocytized CA of conspicuous and inconspicuous groups (n=100 each), and intact ones (n=200) were measured individually using a microscope equipped with graticule, and analyzed by Student’s t-test. Cases 2, 5, 6 and 9 were employed for this purpose because of abundance of phagocytized as well as intact CA. The intact CA located in anatomically equivalent neighboring areas were chosen and measured for this purpose to reduce sampling bias. Alteration of the distribution density and pattern of CA in each affected area were also assessed qualitatively in comparison with the anatomically corresponding neighboring uninvolved area.

RESULTS

Based on neuropathological and immunohistochemical examination, 57 lesions were recognized. The classification of lesion patterns (A-F)⁸ is summarized in Table 3. Three of the 57 lesions showed pattern A, 11 pattern C, 15 pattern D, 6 pattern E, and 22 pattern F. There were no lesions with simultaneous loss of AQP4, GFAP and MBP expression (pattern B). The loss of AQP4 was seen in 29 of 57 lesions, while complete loss of GFAP staining was found in only 3. Immunoreactivity of MBP was partially restored in 36 lesions (patterns A, C and F), but completely lost in 21 (patterns D and E). There was no apparent correlation between MBP expression and clinical duration or disease activity. In actively demyelinating lesions, lipid-laden macrophages infiltrated diffusely, and immunoreactivity to AQP4 was completely lost. Although GFAP expression was relatively preserved, GFAP-positive astrocytes were reduced in number and showed fewer and shorter processes, especially in lesions with numerous macrophage infiltrations. These lesions were mostly classified into pattern C or D. In case 9, showing the shortest clinical course (27 days), all lesions were pattern C (AQP4-negative, GFAP-slightly positive, MBP-positive). In chronic active lesions with mild macrophage infiltration with occasional cystic change, the expression of AQP4 and GFAP tended to be preserved, or more precisely, recovered (patterns E and F). All lesions in case 6, the longest survivor (40 years) among our 9 cases, were pattern F (AQP4-positive, GFAP-positive, MBP-positive). These were old lesions extensively replaced by fibrosis and scattered macrophages devoid of inflammatory cell infiltration. Lesions with preserved immunoreactivity of MBP and loss of AQP4 and GFAP (pattern A) were seen only in the thoracic spinal cord of case 8 with a long clinical course (33 years). These were hypocellular inactive old lesions replaced either by fibrosis or remyelinating Schwann cells

sprouting from the entry zone of the dorsal root. They might not be true pattern A, which was perhaps intended as lesions with acute astrocyte loss.⁸ The remyelinated area was stained by the antibodies to Schwann/2E as well as MBP. The large remyelinated area displayed pattern A, while the surrounding fibrous area was pattern F. Remyelination by Schwann cells was also observed in chronic old lesions in other cases, but confined to smaller areas.

Thus, it was confirmed that all 9 cases possessed NMO lesions of various temporal phases. The pathology of CA was analyzed on the basis of morphological observation. Firstly, the morphology as well as distribution of CA in unaffected areas was evaluated, and confirmed to be usual. They were likely to be seen in the subpial and perivascular position, where the immunopositivity of AQP4 colocalized (Fig. 1A, B). Phagocytized CA were recognized in 8 of 9 cases (except case 8), and in 42 of 57 (74%) lesions. In some active demyelinating lesions in cases 3, 4 and 9 (5 lesions in total), CA-laden macrophages were abundantly seen by HE staining (i.e., conspicuous lesions) (Fig. 2A-D). Among them, macrophages engulfing two or more CA were often encountered (Fig. 2D inset). Occasionally, PAS-positive granular debris was seen in the cytoplasm, indicating digestive process of phagocytized CA (Fig. 2E). The areas containing conspicuous lesions were classified into either pattern C (cases 3 and 4) or D (case 9) (Table 4). Also, in many other lesions, phagocytized CA could be recognized by CD68-PAS double staining (i.e., inconspicuous lesions) (Fig. 2F, G). Phagocytized CA of inconspicuous groups were likely to be seen in inactive lesions, and the distribution density was essentially lower than that of conspicuous groups. Only case 8 did not possess phagocytized CA in any lesions, which were predominantly composed of old,

burned-out lesions with no apparent inflammatory reaction. There was no apparent regional difference (i.e., optic nerve, medulla, spinal cord) regarding CA phagocytization. It should be remarked that phagocytized figures were restricted to affected areas, and they were never seen in uninvolved areas (Fig. 2H), and the number of CA in intact areas was essentially retained.

Alteration of the number of CA could be assessed in 35 out of 57 lesions. Twenty two lesions were excluded in this study, the reason of most cases being impossibility of setting appropriate controls. In 26 of 35 lesions, the number of CA was clearly fewer in comparison to the neighboring uninvolved area (Fig. 3). In 4 chronic old lesions (1 in case 6 and 3 in case 8, all classified as pattern F), phagocytized as well as intact CA disappeared totally, while CA were distributed normally in the adjacent uninvolved areas.

Since phagocytized CA were seemingly smaller and fragmentary, quantitative analysis was performed. The average diameter of intact CA (average \pm standard deviation (μm), 12.22 ± 3.34) was significantly larger than that of phagocytized CA of the conspicuous (10.15 ± 3.34) ($p<0.0001$) and inconspicuous (7.16 ± 2.36) ($p<0.0001$) groups, respectively (Fig. 4).

DISCUSSION

The discovery of a specific antibody to AQP4 in NMO patients has led to a great advance in research on the disease.^{5,6} NMO is presumed to be an antibody-mediated disorder, the major target antigen being AQP4 on astrocytic membrane, although a small number of AQP4-negative NMO exists. Regions susceptible to NMO tend to express higher levels of AQP4 and/or be devoid of a

blood-brain barrier, such as the vascular endfeet of astrocytic processes, the optic nerve, the spinal cord, and circumventricular organs.^{1,2} According to recent studies, damaged astrocytes in the disease process lose their ability to uptake and catalyze glutamate, an excitotoxic amino acid, eventually leading to injury of oligodendrocytes and neurons in the vicinity.^{11,25} Early loss of AQP4 and GFAP immunoreactivity in the affected areas prior to MBP loss^{7,8} and remarkable elevation of GFAP and S100 β in CSF¹⁵⁻¹⁷ are supportive neuropathological and clinical observations of NMO as a primary astrocytopathy.

As mentioned earlier, we observed a case of rapidly-progressive NMO spectrum disorder that displayed abundant phagocytized CA in the CNS lesion.¹⁹ CA are glycoproteinaceous inclusions chiefly located within astrocytic processes around blood vessels and in the subependymal and subpial spaces. They are basically physiological structures and accumulate in association with aging.^{20,26} In Lafora's disease, polyglucosan bodies (Lafora bodies) are found in neuronal cytoplasm. They closely resemble CA, and are stained intensely with PAS like CA.²⁰ Increased numbers of CA were also found in association with several neurological conditions such as Alzheimer's disease, multiple sclerosis and mesial temporal sclerosis.²⁶⁻²⁸

In this study, we expanded the subject (57 lesions in 9 cases) to clarify the significance of CA phagocytization in NMO. We classified the NMO lesions based primarily on AQP4, GFAP and MBP immunohistochemistry, instead of previous qualitative staging occasionally used commonly for NMO and MS.⁸ Detailed neuropathological investigation uncovered diverse NMO lesions of various activities and temporal phases. The expression of AQP4 and GFAP tended to be diminished or lost, whereas MBP was relatively preserved in early

active lesions. These findings suggested that astrocytes were primarily involved in NMO lesions, consistent with previous reports.^{7,8} A considerable reduction of GFAP immunoreactivity was frequently seen in early active lesions; however, complete loss was rare in this study. Our anti-GFAP antibody was rabbit polyclonal raised against the whole protein,²² the high sensitivity of which has been demonstrated in a number of our previous studies.²⁹ In chronic lesions, both AQP4 and GFAP tended to be spared, possibly because of tissue repair by reactive astrocytes.

CA-bearing macrophages were demonstrated in 42 lesions in 8 cases, while they were not seen in intact areas. Phagocytized CA in conspicuous groups were confined to active lesions, while those of inconspicuous groups were likely to be seen in inactive lesions. The other macrophage markers, such as Iba-1 (Wako, Osaka, Japan), KP1, and PGM1 (DAKO), were tested in selected cases, and depicted phagocytizing figures similar to Ki-M1P (data not shown). In either case, immunopositivity for AQP4 and GFAP was lost or diminished, indicating coincident astrocytic injury in the lesions. Additionally, the size of phagocytized CA was significantly smaller than that of intact CA, and the CA were generally fewer in affected areas. We assume that the observation essentially results in CA phagocytization; however, possibility remains that CA have increased in peri-inflammatory area. Since the size and number of CA tends to increase with age, however, considerable diversity exists even in age-matched conditions.²⁶ Moreover, anatomical location (*eg*, gray vs. white matter) affects the CA size in each individual case,²⁶ so we considered the best normal controls for the phagocytized CA to be those located in anatomically equivalent neighboring areas. On the basis of our observation, the following

process was strongly suggested: CA were torn from damaged astrocytes in the disease process, recognized as foreign bodies by the local immune system, and engulfed and digested by macrophages.

Indeed, phagocytized CA are rarely encountered in brain tumors or infarction (unpublished observation); however, to our knowledge, no systematic analyses of phagocytized CA in neurological disorders have been reported. It remains to be clarified why phagocytized CA frequently appear in NMO. AQP4, a presumed target antigen of NMO, is mainly distributed on astrocyte cell processes, where CA coexist. These CA may be a target of phagocytosis in the earlier stage of brain injury. In addition to simple foreign body reactions caused by astrocytic injury and concomitant CA release, it is speculated that the autoantibody and complements possibly studded on CA may mediate and promote immune reactions. In an earlier study, granulocytes attracted by complements, natural killer cells, and antibody-dependent cellular cytotoxicity suggested to be involved in tissue injury in NMO.³⁰

It is widely accepted that CA accumulate in the brain with aging; however, the exact rate is unknown. Nonetheless, it appears to be very slow, and once the CA are removed, it surely takes a considerably long time for reconstruction. In our observation, the period seemed to be longer than that for the growth of reactive astrocytes. Therefore, loss of CA is a better histopathological indicator of past astrocytic injury in NMO.

It is of interest to understand to what extent a phagocytized figure of CA is pathognomonic in order to differentiate NMO from other demyelinating disorders, and it remains to be elucidated. It is of note that Singhrao et al. demonstrated the increase of CA in MS quantitatively,²⁸ suggesting that NMO

and MS pursue essentially different pathological courses, and the morphological state of CA can be an indicator for neuropathological differential diagnosis between them.

In conclusion, we confirmed the frequent advent of phagocytized CA in NMO, and the following pathophysiological process of NMO is presumed on the basis of our observation: the astrocytes are primarily affected in NMO lesions, and CA discharged from astrocytes are phagocytized by macrophages; thereafter destroyed tissue is repaired by reactive astrogliosis. Thus, a phagocytized figure and resultant disappearance of CA can be a new histological hallmark of astrocytic injury in NMO, recognizable even on plain HE specimens.

ACKNOWLEDGEMENT

The authors are grateful to Mr. Koji Isoda (Gunma University) for his excellent technical assistance.

REFERENCES

1. Jacob A. Neuromyelitis optica - an update: 2007-2009. *Ann Indian Acad Neurol* 2009; **12**: 231-237.
2. Hinson SR, McKeon A, Lennon VA. Neurological autoimmunity targeting aquaporin-4. *Neuroscience* 2010; **168**: 1009-1018.
3. Misu T, Fujihara K, Nakashima I *et al*. Pure optic-spinal form of multiple sclerosis in Japan. *Brain* 2002; **125**: 2460-2468.
4. Kira J. Multiple sclerosis in the Japanese population. *Lancet Neurol* 2003; **2**: 117-127.
5. Lennon VA, Wingerchuk DM, Kryzer TJ *et al*. A serum autoantibody marker of neuromyelitis optica: distinction from multiple sclerosis. *Lancet* 2004; **364**: 2106-2112.
6. Lennon VA, Kryzer TJ, Pittock SJ, Verkman AS, Hinson SR. IgG marker of optic-spinal multiple sclerosis binds to the aquaporin-4 water channel. *J Exp Med* 2005; **202**: 473-477.
7. Roemer SF, Parisi JE, Lennon VA *et al*. Pattern-specific loss of aquaporin-4 immunoreactivity distinguishes neuromyelitis optica from multiple sclerosis. *Brain* 2007; **130**: 1194-1205.
8. Misu T, Fujihara K, Kakita A *et al*. Loss of aquaporin 4 in lesions of neuromyelitis optica: distinction from multiple sclerosis. *Brain* 2007; **130**: 1224-1234.

9. Takahashi T, Fujihara K, Nakashima I *et al.* Anti-aquaporin-4 antibody is involved in the pathogenesis of NMO: a study on antibody titre. *Brain* 2007; **130**: 1235-1243.
10. Watanabe S, Nakashima I, Misu T *et al.* Therapeutic efficacy of plasma exchange in NMO-IgG-positive patients with neuromyelitis optica. *Mult Scler* 2007; **13**: 128-132.
11. Hinson SR, Roemer SF, Lucchinetti CF *et al.* Aquaporin-4-binding autoantibodies in patients with neuromyelitis optica impair glutamate transport by down-regulating EAAT2. *J Exp Med* 2008; **205**: 2473-2481.
12. Kinoshita M, Nakatsuji Y, Moriya M *et al.* Astrocytic necrosis is induced by anti-aquaporin-4 antibody-positive serum. *Neuroreport* 2009; **20**: 508-512.
13. Kinoshita M, Nakatsuji Y, Kimura T *et al.* Neuromyelitis optica: Passive transfer to rats by human immunoglobulin. *Biochem Biophys Res Commun* 2009; **386**: 623-627.
14. Bradl M, Misu T, Takahashi T *et al.* Neuromyelitis optica: pathogenicity of patient immunoglobulin in vivo. *Ann Neurol* 2009; **66**: 630-643.
15. Misu T, Takano R, Fujihara K, Takahashi T, Sato S, Itoyama Y. Marked increase in cerebrospinal fluid glial fibrillar acidic protein in neuromyelitis optica: an astrocytic damage marker. *J Neurol Neurosurg Psychiatry* 2009; **80**: 575-577.

16. Takano R, Misu T, Takahashi T, Sato S, Fujihara K, Itoyama Y. Astrocytic damage is far more severe than demyelination in NMO: a clinical CSF biomarker study. *Neurology* 2010; **75**: 208-216.
17. Petzold A, Marignier R, Verbeek MM, Confavreux C. Glial but not axonal protein biomarkers as a new supportive diagnostic criteria for Devic neuromyelitis optica? Preliminary results on 188 patients with different neurological diseases. *J Neurol Neurosurg Psychiatry* 2011; **82**: 467-469.
18. Wingerchuk DM, Lennon VA, Lucchinetti CF, Pittock SJ, Weinshenker BG. The spectrum of neuromyelitis optica. *Lancet Neurol* 2007; **6**: 805-815.
19. Goshima A, Matsumura N, Yokoo H, Nakazato Y, Harigaya Y, Itoh H. Acute necrotizing medullomyelitis (abortive form of neuromyelitis optica) showing considerable loss of astrocytes and phagocytosis of corpora amylacea. An autopsy report. (Abstract) *Neuropathology* 2010; **30**: 118.
20. Love S, Louis DN, Ellison DW. *Greenfield's neuropathology, eighth edition*. London, UK: Hodder Arnold 2008.
21. Ikota H, Iwasaki A, Kawarai M, Nakazato Y. Neuromyelitis optica with intraspinal expansion of Schwann cell remyelination. *Neuropathology* 2010; **30**: 427-433.
22. Nakazato Y, Ishizeki J, Takahashi K, Yamaguchi H, Kamei T, Mori T. Localization of S-100 protein and glial fibrillary acidic protein-related antigen in pleomorphic adenoma of the salivary glands. *Lab Invest* 1982; **46**: 621-626.

23. Arai H, Hirato J, Nakazato Y. A novel marker of Schwann cells and myelin of the peripheral nervous system. *Pathol Int* 1998; **48**: 206-214.
24. Bruck W, Porada P, Poser S *et al.* Monocyte/macrophage differentiation in early multiple sclerosis lesions. *Ann Neurol* 1995; **38**: 788-796.
25. Marignier R, Nicolle A, Watrin C *et al.* Oligodendrocytes are damaged by neuromyelitis optica immunoglobulin G via astrocyte injury. *Brain* 2010; **133**: 2578-2591.
26. Cavanagh JB. Corpora-amylacea and the family of polyglucosan diseases. *Brain Res Rev* 1999; **29**: 265-295.
27. Chung MH, Horoupian DS. Corpora amylacea: a marker for mesial temporal sclerosis. *J Neuropathol Exp Neurol* 1996; **55**: 403-408.
28. Singhrao SK, Morgan BP, Neal JW, Newman GR. A functional role for corpora amylacea based on evidence from complement studies. *Neurodegeneration* 1995; **4**: 335-345.
29. Yokoo H, Tanaka Y, Nobusawa S, Nakazato Y, Ohgaki H. Immunohistochemical and ultrastructural characterization of brain tumors in S100 β -v-erbB transgenic rats. *Neuropathology* 2008; **28**: 591-598.
30. Vincent T, Saikali P, Cayrol R *et al.* Functional consequences of neuromyelitis optica-IgG astrocyte interactions on blood-brain barrier permeability and granulocyte recruitment. *J Immunol* 2008; **181**: 5730-5737.

Figure Legends

Fig. 1. Corpora amylacea (CA) in unaffected regions of neuromyelitis optica (NMO) (case 9). The sections are doubly stained with aquaporin-4 (AQP4) and periodic acid-Schiff (PAS). The intact CA are likely to be seen in subpial (**A**, medulla oblongata) and perivascular (**B**, thoracic spinal cord) AQP4-positive areas. Bar=50 μ m

Fig. 2. CA in NMO-affected regions. **A** Optic nerve of case 5. Phagocytized CA are recognizable by hematoxylin and eosin (HE)-stained section. CA are likely to be collected within infiltrating macrophages. **B** Adjacent area of **A** doubly stained with CD68 and PAS displays CA-laden macrophages more clearly. **C** Medulla oblongata of case 9. Abundant phagocytized CA are seen in the subependymal area by HE specimen. **D** CD68-PAS specimen adjacent to **C**. Macrophages containing two or more CA are occasionally seen (inset). **E** AQP4-PAS specimen adjacent to **C** and **D**. CA engulfed by macrophages are located in AQP4-negative area. PAS-positive granular debris is seen in the cytoplasm (left lower area), indicating digestive process of phagocytized CA. **F**, **G** Phagocytized CA recognized only by CD68-PAS specimens. The size is seemingly smaller and variegated. (**F**: thoracic spinal cord of case 3, **G**: medulla oblongata of case 7). Bar in **A-G** =50 μ m. **H** Distribution of phagocytized CA in the medulla oblongata (case 9) plotted on an AQP4-immunostained specimen. Each dot represents one phagocytized CA. It is of note that phagocytized CA are found only in the AQP4-negative affected area, and never seen in an uninvolved area.

Fig. 3 Medulla oblongata of case 7 with AQP4-PAS staining. The number of CA in the affected area (right) is clearly fewer in comparison to the neighboring uninvolved area (left). Note that AQP4 immunostaining is rather enhanced in the affected area, indicating reactive astrocytosis. Bar = 500 μ m.

Fig. 4. Statistical analysis of the size of CA. The diameter of intact CA (n=200), phagocytized CA noticeable by HE specimens (i.e., conspicuous group) (n=100), and those only recognized by CD68-PAS specimens (i.e., inconspicuous group) (n=100) are measured and plotted. By Student's t-test, the diameter of phagocytized CA has been demonstrated to be significantly smaller than that of intact CA. In particular, those of inconspicuous groups are much smaller, suggesting a more advanced stage of digestion. Ave: average size, SD: standard deviation.

Table 1. Case list of neuromyelitis optica spectrum disorder.

case	age(y)/sex	duration of illness	brain weight (g)
1	80/M	9m	1105
2	77/M	3m	1275
3	67/F	3y	1270
4	80/F	13y	870
5	47/M	27y	nd
6	79/M	40y	1115
7	64/F	8y	1060
8	69/F	33y	nd
9	66/M	27d	1455

M: male, F: female, d: day, m: month, y: year, g: gram, nd: no data.

Table 2. Histological classification (patterns A-F) of neuromyelitis optica lesion based on expression pattern of aquaporin-4 (AQP4), glial fibrillary acidic protein (GFAP) and myelin basic protein (MBP) by Misu et al. [17].

	A	B	C	D	E	F
AQP4	-	-	-	-	+	+
GFAP	-	-	+	+	+	+
MBP	+	-	+	-	-	+

+: at least partially preserved immunoreactivity

-: complete loss of immunoreactivity

Table 3. Details of lesion pattern in each case.

case	number of lesions assessed	lesion pattern					
		A	B	C	D	E	F
1	10			5	2	1	2
2	2				1		1
3	11			2	4	2	3
4	3					2	1
5	7				5		2
6	6						6
7	8				3	1	4
8	6	3					3
9	4			4			
Total	57	3	0	11	15	6	22

The definitions of patterns A – F are shown in Table 2.

Table 4. Expression pattern and phagocytized CA in each lesion.

extent of phagocytosis	lesion pattern						total
	A	B	C	D	E	F	
conspicuous			3	2			5
inconspicuous			4	13	3	17	37
absent	3		6		1	5	15

Conspicuous: lesions with phagocytic macrophages recognizable by HE staining.

Inconspicuous: lesions with phagocytic macrophages recognized by CD68-PAS staining.

Fig. 1

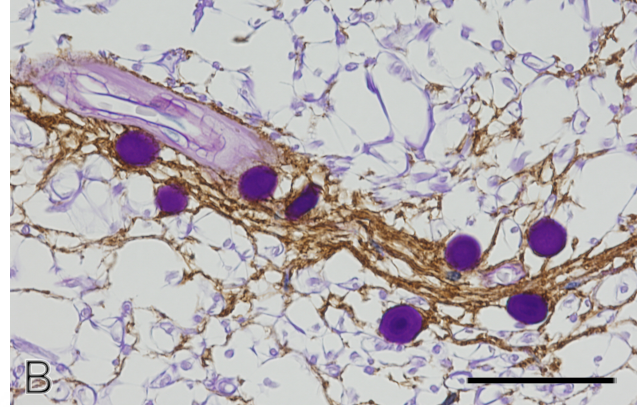
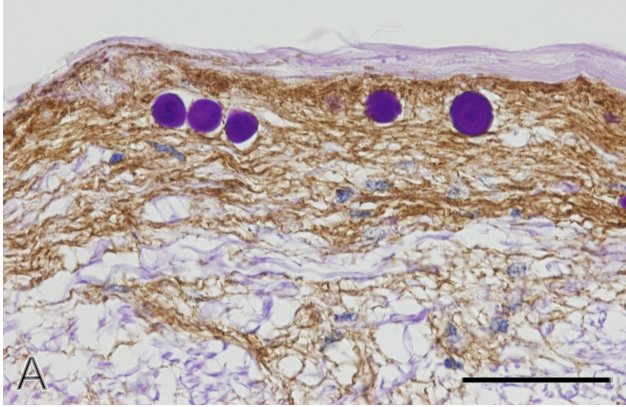


Fig. 2

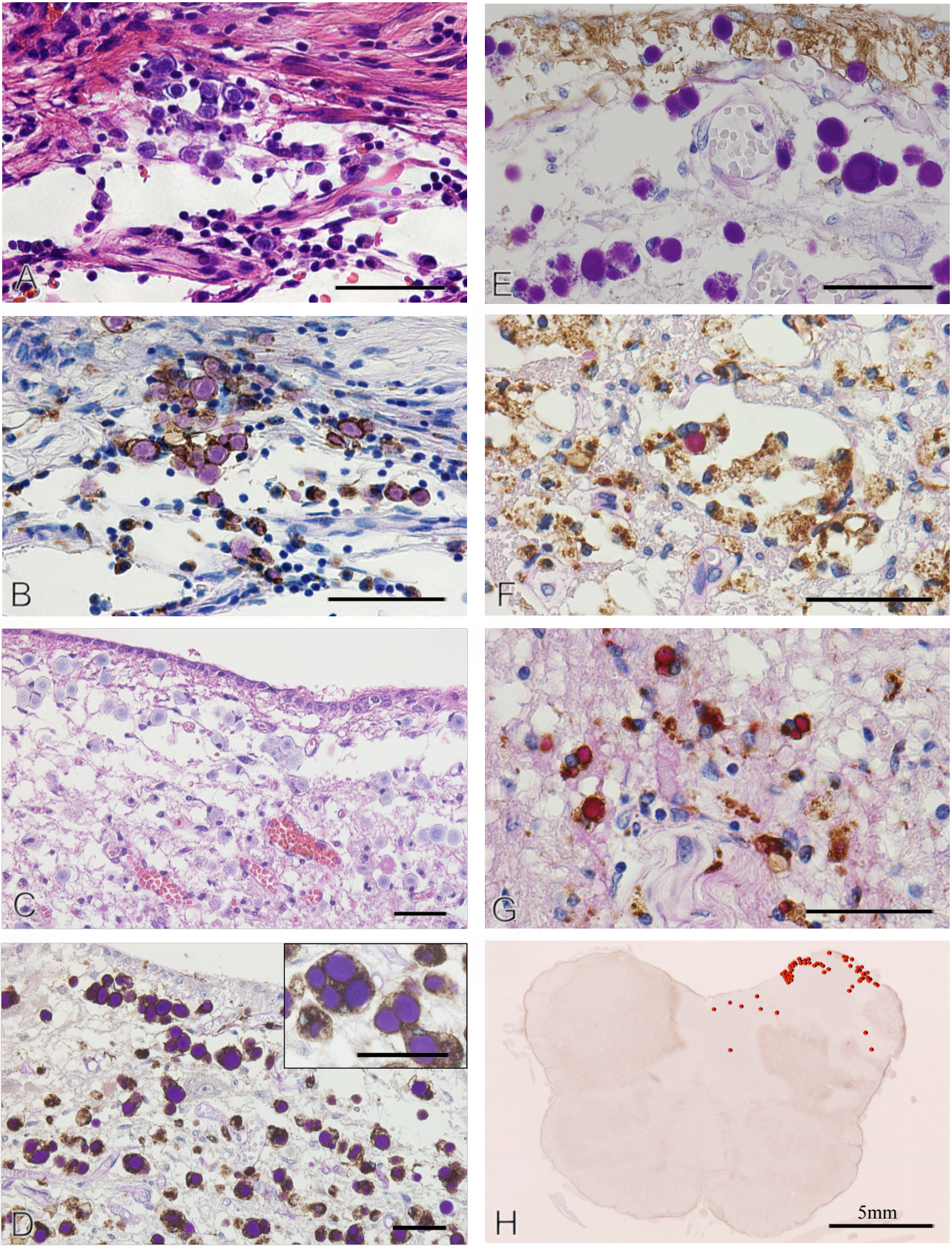


Fig. 3

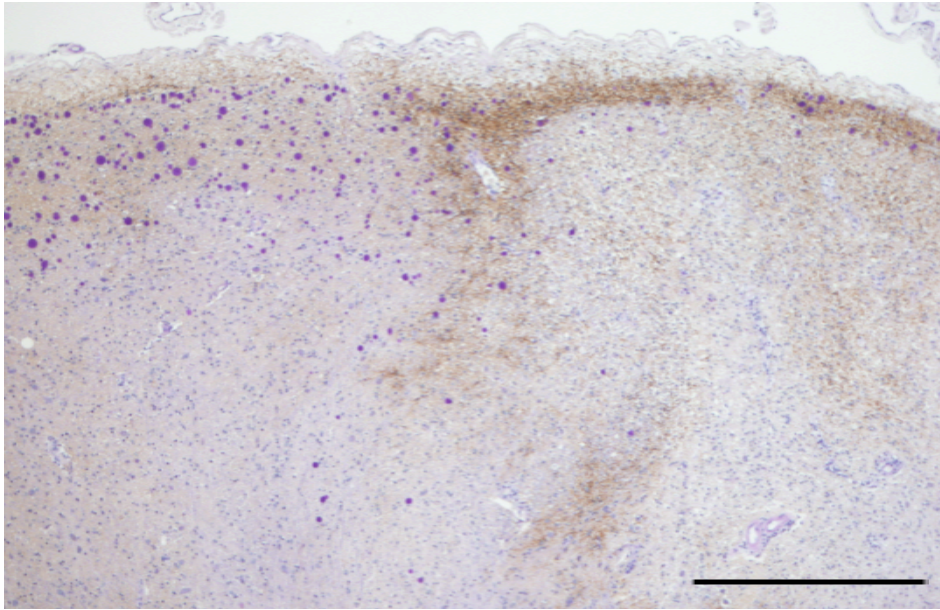


Fig. 4

